Magnetically Driven Metal-Insulator Transition in $NaOsO_3$

S. Calder,[1,*] V. O. Garlea,[1] D. F. McMorrow,[2] M. D. Lumsden,[1] M. B. Stone,[1] J. C. Lang,[3] J.-W. Kim,[3] J. A. Schlueter,[4] Y. G. Shi,[5,6] K. Yamaura,[6] Y. S. Sun,[7] Y. Tsujimoto,[7] and A. D. Christianson[1]

[1]*Quantum Condensed Matter Division, Oak Ridge National Laboratory, Oak Ridge, Tennessee 37831, USA*
[2]*London Centre for Nanotechnology, University College London, London, WC1H 0AH, United Kingdom*
[3]*Advanced Photon Source, Argonne National Laboratory, Argonne, Illinois 60439, USA*
[4]*Materials Science Division, Argonne National Laboratory, Argonne, Illinois 60439, USA*
[5]*Institute of Physics, Chinese Academy of Sciences, 100190 Beijing, China*
[6]*Superconducting Properties Unit, National Institute for Materials Science, 1-1 Namiki, Tsukuba, 305-0044 Ibaraki, Japan*
[7]*International Center for Materials Nanoarchitectonics (WPI-MANA), National Institute for Materials Science, Tsukuba, Ibaraki 305-0044, Japan*

(Received 7 February 2012; revised manuscript received 21 March 2012; published 21 June 2012)

The metal-insulator transition (MIT) is one of the most dramatic manifestations of electron correlations in materials. Various mechanisms producing MITs have been extensively considered, including the Mott (electron localization via Coulomb repulsion), Anderson (localization via disorder), and Peierls (localization via distortion of a periodic one-dimensional lattice) mechanisms. One additional route to a MIT proposed by Slater, in which long-range magnetic order in a three dimensional system drives the MIT, has received relatively little attention. Using neutron and x-ray scattering we show that the MIT in $NaOsO_3$ is coincident with the onset of long-range commensurate three dimensional magnetic order. While candidate materials have been suggested, our experimental methodology allows the first definitive demonstration of the long predicted Slater MIT.

DOI: 10.1103/PhysRevLett.108.257209 PACS numbers: 75.10.Lp, 71.30.+h, 75.25.−j, 75.70.Tj

The precise microscopic origin behind metal-insulator transitions (MITs) has been one of the enduring problems within condensed matter physics [1]. Many materials exhibit a Mott MIT that is explained by invoking strong Coulomb interactions (U) which open a gap at the Fermi energy forcing the conductor into an insulating phase [2,3]. A Mott MIT is independent of magnetic correlations. One alternative route to a MIT, known as the Slater transition, is driven by antiferromagnetic (AFM) order alone, opening a band gap independent of strong U [4]. Although magnetism is often present in the phase diagram of a MIT, there have been no definitive experimental examples of a three dimensional (3D) magnetically driven Slater MIT.

The $5d$ transition metal oxide $NaOsO_3$ [5], along with $Cd_2Os_2O_7$ [6–9] and $Ln_2Ir_2O_7$ (Ln = Lanthanide) [10,11], have been suggested on the basis of bulk measurements to host a Slater MIT. However, to define a material as undergoing a Slater MIT it is obligatory to show microscopic 3D commensurate long-range magnetic ordering concurrent with the MIT. There exists no such experimental evidence in any candidate material. For $Cd_2Os_2O_7$ and $Ln_2Ir_2O_7$ the elusiveness of an experimental verification can be attributed to the inherent magnetic frustration in the pyrochlore lattice and prohibitively high neutron absorption values for Cd and Ir. We have investigated the continuous MIT in $NaOsO_3$ with neutron and x-ray scattering, observed long-range magnetic order at the MIT, and determined the nature of that order on a microscopic level, thus presenting the first definitive experimental example of a Slater MIT.

Slater's description of a magnetically driven MIT is shown schematically in Fig. 1. Commensurate AFM order, with every neighboring spin oppositely aligned, occurs at the MIT temperature (T_{MIT}) creating an opposite periodic

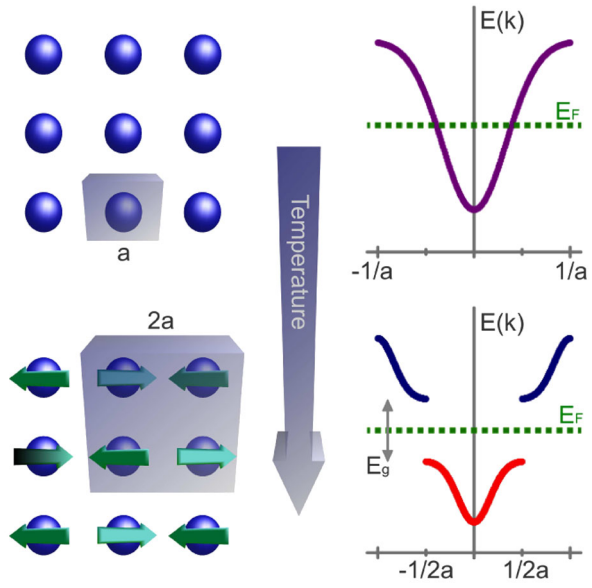

FIG. 1 (color online). Slater MIT. (Left) commensurate AFM order doubles the unit cell. (Right) Simplified band structure. The opposite potential on each neighboring ion in the magnetic regime splits the electronic band, creating an insulating band gap.

potential on each nearest neighbor. This results in an energy gap that splits the electronic band at the newly created magnetic Brillouin zone boundary. In a half-filled electronic outer level the lower band will be preferentially fully occupied and the upper band empty. The emergence of this band gap causes the system to undergo a Slater MIT, and provides a canonical example of an itinerant system that can be described by the self-consistent single electron Hartree-Fock theory [12].

Single crystal ($0.2 \times 0.2 \times 0.05$ mm) and polycrystalline (4.6 g) samples of $NaOsO_3$ were prepared in pressures up to 6 GPa as described in Ref. [5]. Neutron powder diffraction (NPD) was performed at the High Flux Isotope Reactor (HFIR) using beam line HB-2A with a wavelength of $\lambda = 1.54$ Å. The results were Rietveld refined with FULLPROF and representational analysis performed using SARAh [13]. Polarized and unpolarized elastic measurements were performed on the spectrometer HB-1 at HFIR with $\lambda = 2.46$ Å. Polarization was performed using a vertical focusing Heussler monochromator with a vertical guide field with a flipping ratio of 14. Magnetic resonant x-ray scattering (MRXS) was carried out at beam line 6-ID-B at the Advanced Photon Source (APS). Graphite was used as the polarization analyzer crystal at the (0,0,10) and (0,0,8) reflections on the $L2$ and $L3$ edges, respectively, to achieve a scattering angle close to 90°. To account for absorption, energy scans were performed without the analyzer and with the detector away from any Bragg peaks at both edges.

A first-order structural transition is often associated with a Mott MIT; however this should not occur in the continuous Slater MIT. To test this we performed NPD through $T_{MIT} \approx 410$ K of $NaOsO_3$ from 200 to 500 K. The results were refined to a structural model of a distorted perovskite structure with space group *Pnma*, in agreement with the results in Ref. [5]. We note that χ^2 remained consistent for all temperatures with a range of $2.29 \leq \chi^2 \leq 3.29$ (see the Supplemental Material [14] for a complete set of refinement parameters). Taken along with the smooth thermal shifting of Bragg peaks observed strongly indicates that the *Pnma* structural model is equally applicable, and correct, above and below T_{MIT}.

The temperature variation of the parameters from NPD for $NaOsO_3$ are shown in Fig. 2. The unit cell volume shows no deviation through T_{MIT}, with the small expansion of under 0.1% indicative of a stable crystal structure [Fig. 2(a)]. The anomaly observed in the a and c axis at T_{MIT} [Fig. 2(b)] is not an indication of a structural symmetry change or unstable structure, as evidenced by the stable thermal parameters through T_{MIT} in Fig. 2(c). Instead the a-c structural behavior can be understood by considering the ions that control the lattice constants, namely the Os-Os bond distance [Fig. 2(d)] and Os-O2-Os bond angle [Fig. 2(e)]. To relieve tension and reduce energy the distorted octahedra prefer to align with the unit

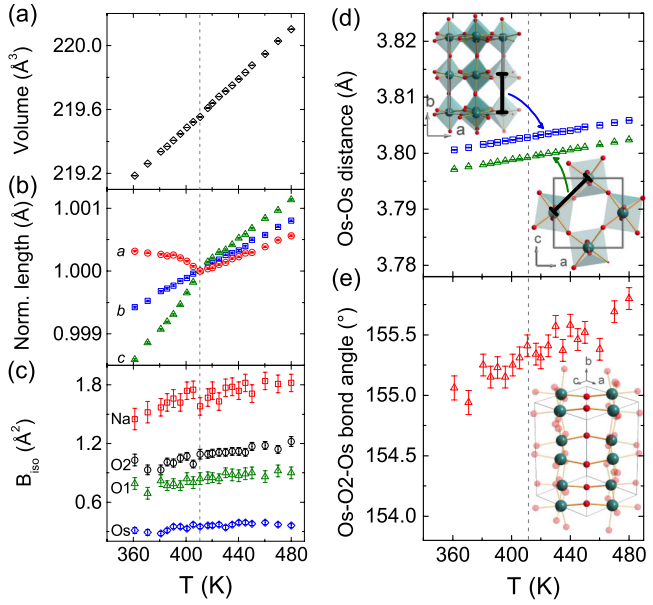

FIG. 2 (color online). Refined structural parameters from NPD. The vertical dashed line indicates T_{MIT}. The insets of (d) and (e) are a representation of the crystallographic bond lengths and angles considered, with the larger spheres indicating the Os ions and the small spheres indicating the oxygen ions. The crystal structure shows an anomaly in the a and c lattice constants at T_{MIT}. However, there is no indication of a structural symmetry change.

cell axis as the temperature is lowered, resulting in the Os-O2-Os bond angle decreasing. This bond is overwhelmingly along the a and c directions and as such a change in the Os-O2-Os bond angle results in a change in the a and c unit cell lengths, as observed. Consequently the Os ions along the a-c axis are pulled closer together. When sufficiently close, the Os ions interact and form the magnetic long-range ordered phase observed. This suggests a magnetostriction control parameter in which it would be possible to influence T_{MIT} by controlling the a-c unit cell lengths with pressure.

Additional Bragg peaks develop below T_{MIT} in the NPD pattern in Figs. 3(a) and 3(b), indicative of magnetic order. Measuring the commensurate peak at $|Q| \approx 1.43$ Å^{-1}, consistent with the (110) and (011) reflections, with polarized neutrons unambiguously assigns the additional scattering below T_{MIT} as arising from magnetic order [see Fig. 3(c)]. To determine the nature of the magnetic order we implemented representational analysis [13]. For a second order transition, Landau theory states that the symmetry properties of the magnetic structure are described by only one irreducible representation. For the *Pnma* crystal structure with the magnetic moment on the Os ion and commensurate propagation vector $\mathbf{k} = (000)$, there are four possible irreducible representations. Only one gave a correct description of the magnetic scattering intensities in $NaOsO_3$, labelled $\Gamma(5)$ (following the numbering scheme

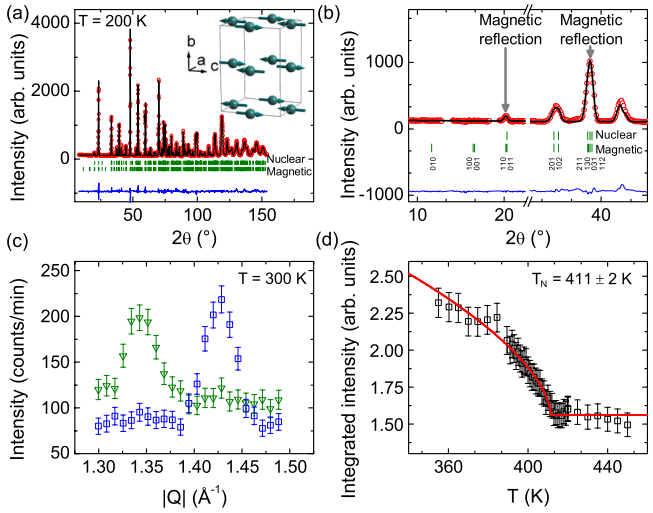

FIG. 3 (color online). (a)–(b) NPD modeled with crystallographic space group *Pnma* and *G*-type AFM ordering. Magnetic order is shown schematically inset, with only the Os ions represented for clarity. (c) Polarized NPD with polarization parallel to the scattering vector with flipper-on (triangles) and flipper-off (squares) unambiguously assigns the scattering centered around $|Q| = 1.43$ Å^{-1} as purely magnetic. The lower $|Q| \approx 1.35$ Å^{-1} structural peak corresponds to an unknown non-magnetic impurity phase. (d) Integrated intensity of the $|Q| = 1.43$ Å^{-1} peak as a function of temperature. The solid line is a power law fit as described in the text.

of Kovalev). This is equivalent to the Shubnikov group $Pn'ma'$ or A_x, F_y, G_z according to Bertaut's notation. Only scattering from spins along the *c*-axis produced intensities at the correct reflections, as shown by the fits in Figs. 3(a) and 3(b).

We have thus established $NaOsO_3$ to have AFM long-range order, with the spins oriented along the *c* axis in the *G*-type AFM structure with every nearest neighboring spin oppositely aligned, shown schematically in Fig. 3(a). A survey of specific Bragg peaks (polarized and unpolarized) through the magnetic transition revealed no evidence for canting of the spins along either the *a* or *b* axis that would be indicated by additional Bragg peaks compatible with the $\Gamma(5)$ irreducible representation.

Figure 3(d) establishes the AFM transition temperature from the integrated intensity of unpolarized neutron scattering around $|Q| \approx 1.43$ Å^{-1} to be $T_N = 411.(2)$ K with $\beta \approx 0.3(1)$. The scattering is best described as 3D and does not have any of the features necessary to be two dimensional. Therefore AFM order occurs at the same temperature as the change in resistivity, thus linking the AFM-MIT transitions at T_{MIT}, as required for a Slater MIT.

The magnetic moment found from the neutron refinement is 1.0(1) μ_B. This corresponds to an effective moment from the Curie-Weiss (CW) model of $\mu_{\mathrm{eff}} \approx 1.7(1)$ μ_B. While Ref. [5] reported an effective moment of 2.71 μ_B, we note that there are several different temperature regions for which a CW fit can be applied. Considering the different regions, with the inclusion of a diamagnetic correction, provides μ_{eff} values that are consistent with the moment obtained from neutron scattering. A reduced moment is suggestive of the itinerant nature of the 5*d* magnetic ions resulting in a large degree of covalency that is expected in a Slater insulator. However it is also compatible with a breaking of the t_{2g} manifold degeneracy that has been observed in other 5*d* systems due to the large spin-orbit coupling (SOC) [15–17]. The Slater MIT requires a half-filled outer level; therefore splitting of the t_{2g} manifold could lead to incompatibility with the Slater mechanism. To address this we performed MRXS, a technique that selectively measures the enhanced signal at an x-ray absorption edge, allowing a direct probe of the t_{2g} 5*d* electrons in Os^{5+}. Measurements at both the *L*2 edge energy of 10.876 keV, corresponding to a $2p_{(1/2)} \rightarrow 5d$ transition, and the *L*3 edge energy of 12.391 keV ($2p_{(3/2)} \rightarrow 5d$ transition) in Os were undertaken at the (330) and (550) magnetic reflections. The results are shown in Fig. 4 (see the Supplemental Material [14] for measurements through T_{MIT} that support the NPD behavior). The resonant enhancement is approximately

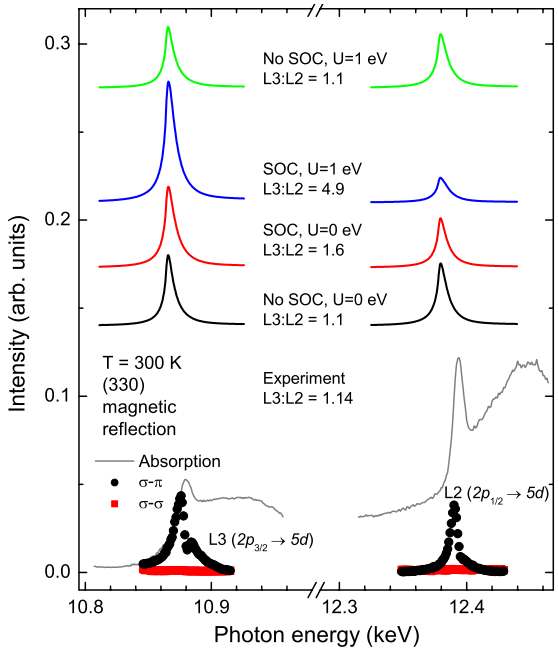

FIG. 4 (color online). Measurement of the resonant enhancement at the *L*2 and *L*3 edges. σ (π) corresponds to polarization perpendicular (parallel) to the scattering plane. The σ-π scattering, sensitive to resonant magnetic scattering, is evident at the expected resonant energies, with a similar enhancement of $\sim 10^2$ at the *L*2 and *L*3 edges. In the σ-σ channel no scattering is observed, showing that the resonant intensity is π polarized, indicating the resonant enhancement is purely from magnetic scattering. The 4 pairs of solid lines in the top portion of the figure are results from FDMNES calculations. No SOC indicates no splitting of the t_{2g} manifold degeneracy, SOC indicates splitting. The ratio of *L*3:*L*2 intensities is shown.

the same at both the $L2$ and $L3$ edges, similar to the observation in another $5d^3$ material [18]. The resonant enhancement at each absorption edge is dependent on transitions between specific electronic levels; therefore splitting of the t_{2g} manifold by SOC or U results in an alteration of the MRXS [18]. We present calculations to reproduce the MRXS scattering using the FDMNES program [19]. FDMNES takes into account SOC and U and has been shown to successfully reproduce MRXS results for $5d$ systems [20]. We ran this *ab initio* program using fully relativistic monoelectronic DFT-LSDA calculations on the basis of Green's formalism for a cluster radius of 2.1 Å. Results are shown as pairs of solid lines at the top of Fig. 4 for both the $L2$ and $L3$ resonant energies. The experimental resonant scattering ratio of edges $L3$:$L2$ is most closely reproduced for the case of no SOC splitting of the t_{2g} manifold and $U = 0$. The addition of SOC into the calculations has the effect of significantly increasing the ratio of $L3$:$L2$ that is not reflected in the experimental results, indicating that SOC does not break the t_{2g} degeneracy. Therefore our MRXS results indicate that the outer t_{2g} manifold is half filled and degenerate, as required for the Slater mechanism and expected for $5d^3$ occupancy [21]. Introducing Coulomb interactions through U decreases the agreement with the experimental MRXS $L2$-edge shape as U increases; this concurs with what would be expected of a Slater MIT in which Coulomb interactions are negligible.

The neutron and x-ray experimental results presented have all the required elements to describe $NaOsO_3$ as undergoing a Slater MIT. We have shown that long-range commensurate AFM order occurs at the same temperature as the continuous MIT. The AFM order is G-type with every nearest neighboring spin oppositely aligned in three dimensions, resulting in an opposite potential surrounding each Os ion in three dimensions that creates an electronic band gap at T_{MIT}. Due to the magnetic Os^{5+} ion having a half-full t_{2g} outer level ($5d^3$), which we have verified from MRXS, the development of this band gap results in a Slater MIT. The t_{2g} degeneracy of single occupied d_{xy}, d_{yz}, and d_{zx} orbitals precludes a structural change through Jahn-Teller distortions. We observed no distortion of the O-Os bond distances and no other evidence for a symmetry change through T_{MIT}. We find a magnetic moment of $\sim 1\ \mu_{\mathrm{B}}$ from neutron scattering. This reduced moment from the expected $S = 3/2$ for Os^{5+} is not due to breaking of the t_{2g} degeneracy by the large SOC, but rather the itinerant nature of $NaOsO_3$ that leads to hybridization between the Os d orbitals and oxygen p orbitals. As an intriguing comparison, a reduced moment and extremely high magnetic ordering temperature of over 1000 K is observed in the $4d$ perovskite $SrTcO_3$ [22], a system that has the same d^3 electron configuration with electron hybridization and strikingly similar magnetic properties to $NaOsO_3$.

The Slater MIT is based on single electron itinerant physics. This contrasts to Mott physics in which strong Coulomb interactions play a central role. This is a key distinction between a magnetically driven MIT being described as a Slater transition or magnetism being simply observed to occur at the Coulomb driven MIT, as is the case in a Mott-Heisenberg transition [12]. Often systems are found to lie in an intermediate regime between Mott (local moment) and Slater (itinerant) systems, and indeed this is an open question in unconventional superconductors. Recent theoretical debate as to the insulating state in the $5d$ system Sr_2IrO_4 underlines this point, with contrasting claims of the role of the Mott and Slater mechanisms in the creation of the insulating state [23,24]. The experimental verification presented allows $NaOsO_3$ to serve as a model system for investigations into the Slater MIT.

We thank B. C. Sales for useful discussions. Work at ORNL was supported by the Scientific User Facilities Division, Office of Basic Energy Sciences, U.S. Department of Energy (DOE). Work at Argonne was supported by the U.S. DOE, Office of Science, Office of Basic Energy Sciences, under contract No. DE-AC02-06CH11357. Research was supported in part by Grant-in-Aid for Scientific Research (22246083, 22850019) from JSPS and FIRST Program from JSPS and ALCA program from JST.

Note added in Proof.—After submission of this work we became aware of a theoretical study of $NaOsO_3$ by Du *et al.* [25] that finds consistent agreement with our experimental results.

*caldersa@ornl.gov

[1] M. Imada, A. Fujimori, and Y. Tokura, Rev. Mod. Phys. **70**, 1039 (1998).
[2] N. F. Mott, Proc. Phys. Soc. London Sect. A **A62**, 416 (1949).
[3] J. Hubbard, Proc. R. Soc. A **276**, 238 (1963).
[4] J. C. Slater, Phys. Rev. **82**, 538 (1951).
[5] Y. G. Shi, Y. F. Guo, S. Yu, M. Arai, A. A. Belik, A. Sato, K. Yamaura, E. Takayama-Muromachi, H. F. Tian, H. X. Yang, J. Q. Li, T. Varga, J. F. Mitchell, and S. Okamoto, Phys. Rev. B **80**, 161104 (2009).
[6] A. W. Sleight, J. L. Gillson, J. F. Weiher, and W. Bindloss, Solid State Commun. **14**, 357 (1974).
[7] D. Mandrus, J. R. Thompson, R. Gaal, L. Forro, J. C. Bryan, B. C. Chakoumakos, L. M. Woods, B. C. Sales, R. S. Fishman, and V. Keppens, Phys. Rev. B **63**, 195104 (2001).
[8] W. J. Padilla, D. Mandrus, and D. N. Basov, Phys. Rev. B **66**, 035120 (2002).
[9] J. Reading and M. T. Weller, J. Mater. Chem. **11**, 2373 (2001).
[10] K. Matsuhira, M. Wakeshima, Y. Hinatsu, and S. Takagi, J. Phys. Soc. Jpn. **80**, 094701 (2011).
[11] S. Zhao, J. M. Mackie, D. E. MacLaughlin, O. O. Bernal, J. J. Ishikawa, Y. Ohta, and S. Nakatsuji, Phys. Rev. B **83**, 180402 (2011).

[12] F. Gebhard, *The Mott Metal-Insulator Transition* (Springer, Berlin, 1997).
[13] A. Wills, Physica (Amsterdam) **276B–278B**, 680 (2000).
[14] See Supplemental Material at http://link.aps.org/supplemental/10.1103/PhysRevLett.108.257209 for crystallographic parameters from 360 to 480 K and a MRXS magnetic order parameter.
[15] B. J. Kim, H. Ohsumi, T. Komesu, S. Sakai, T. Morita, H. Takagi, and T. Arima, Science **323**, 1329 (2009).
[16] D. Pesin and L. Balents, Nature Phys. **6**, 376 (2010).
[17] M. A. Laguna-Marco, D. Haskel, N. Souza-Neto, J. C. Lang, V. V. Krishnamurthy, S. Chikara, G. Cao, and M. van Veenendaal, Phys. Rev. Lett. **105**, 216407 (2010).
[18] D. F. McMorrow, S. E. Nagler, K. A. McEwen, and S. D. Brown, J. Phys. Condens. Matter **15**, L59 (2003).
[19] Y. Joly, Phys. Rev. B **63**, 125120 (2001).
[20] S. Boseggia, R. Springell, H. C. Walker, A. T. Boothroyd, D. Prabhakaran, D. Wermeille, L. Bouchenoire, S. P. Collins, and D. F. McMorrow, arXiv:1201.1452v1.
[21] G. Chen and L. Balents, Phys. Rev. B **84**, 094420 (2011).
[22] E. E. Rodriguez, F. Poineau, A. Llobet, B. J. Kennedy, M. Avdeev, G. J. Thorogood, M. L. Carter, R. Seshadri, D. J. Singh, and A. K. Cheetham, Phys. Rev. Lett. **106**, 067201 (2011).
[23] R. Arita, J. Kunes, A. V. Kozhevnikov, A. G. Eguiluz, and M. Imada, Phys. Rev. Lett. **108**, 086403 (2012).
[24] C. Martins, M. Aichhorn, L. Vaugier, and S. Biermann, Phys. Rev. Lett. **107**, 266404 (2011).
[25] Yongping Du, Xiangang Wan, Li Sheng, Jinming Dong, and Sergey Y. Savrasov, Phys. Rev. B **85**, 174424 (2012).